

# DISTINCTIVE MAGNESIAN, PROTOGRANULAR AND POLYMICT DIOGENITES FROM NORTHWEST AFRICA, OMAN AND UNITED ARAB EMIRATES

T. E. Bunch<sup>1</sup>, A. J. Irving<sup>2</sup>, J. H. Wittke<sup>1</sup>, S. M. Kuehner<sup>2</sup> and D. Rumble, III<sup>3</sup>

<sup>1</sup>Dept. of Geology, Northern Arizona University, Flagstaff, AZ; <sup>2</sup>Dept. of Earth & Space Sciences, University of Washington, Seattle, WA; <sup>3</sup>Geophysical Laboratory, Carnegie Institution, Washington, DC.

## Introduction

Our studies of 36 diogenites collected recently from hot deserts, 32 from Northwest Africa, 1 from Oman and 3 from UAE have revealed new compositional and textural types not previously represented in collections and have important implications for magmatic, metamorphic, and impact mixing processes on 4Vesta. The majority of the specimens resemble classic falls (e. g., Shalka and Johnstown) and finds in that they are brecciated monomict orthopyroxenites composed predominantly of orthopyroxene ( $Fe_{22-31}Wo_{1.3-3.6}$ , FeO/MnO = 25-35 g/g) with accessory chromite, troilite and Ni-poor metal. Several examples contain minor olivine ( $Fe_{25-39}$ ), calcic plagioclase ( $An_{78-96}$ ) and/or clinopyroxene; **NWA 3329** contains minor merrillite and silica. Ten specimens are unbrecciated (*i. e.*, there is no clast rotation), although some minor crushing and veining may be present, and primary textures are mostly intact. We have divided these into 4 orthopyroxenite subtypes based on diagnostic textures and mineralogy.

## Protogranular

This type is best exemplified by the medium-grained **UAE 005** diogenite that has retained most of the original curved to linear igneous grain boundaries (Figure 1). Poikilitic grains are also evident. Other diogenites in this category (below) have experienced various degrees of post-formational textural modifications. **NWA 2037** is similar to UAE 005, but with a wider range in grain size and partial resorption at grain margins. **NWA 1821** has very irregular grain boundaries (Figure 2).

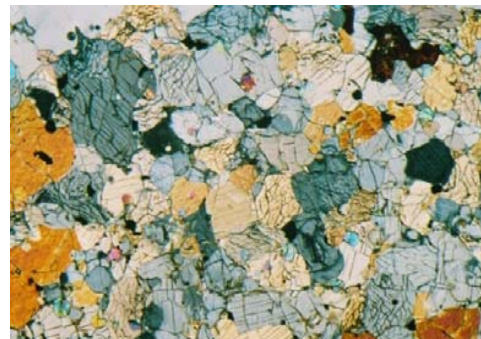


**Figure 1. UAE 005.** Protogranular texture of curved to linear grain boundaries with 96 vol. % orthopyroxene, 3 % chromite, and 1 % olivine. Base width = 7 mm; crossed polarizers.

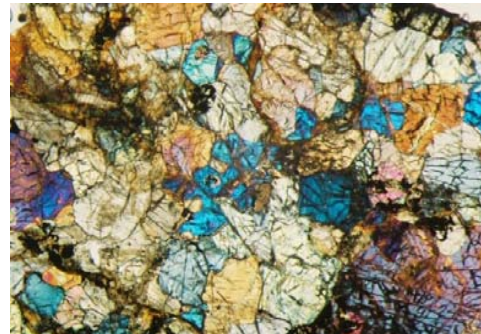


**Figure 2. NWA 2037.** Protogranular texture of variable grain size with less distinct grain boundaries compared with UAE 005. Base width = 9 mm; crossed polarizers.

## Protogranular (Mg-rich)

**NWA 1461** is composed of mostly  $Fe_{13.6}Wo_{0.7}$  orthopyroxene, making it the most magnesian diogenite known (and its pyroxene has the lowest Wo content). This specimen attests to the existence of some very primitive Vestan parent magmas, which also is inferred from the Vestan dunite NWA 2968 [1]. See Figure 3.

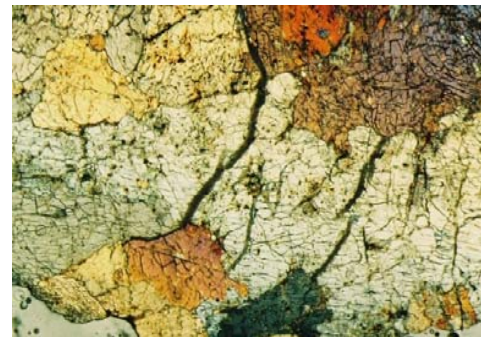


**Figure 3. NWA 1461.** Protogranular texture, with highly irregular, lobate grain boundaries. Base width = 7 mm; cross polarizers.

## Medium to coarse-grained (with corona-like "necklace" around chromites)

**UAE 004** has well-developed linear orientation of orthopyroxene and large, subhedral chromite crystals (< 2.3 mm) with offshoots into the surrounding matrix (Figure 4). Most chromite crystals are surrounded by a necklace-like array of very small anhedral grains of orthopyroxene (orthopyroxene) and olivine (Figure 5). In addition, chromite contains tiny inclusions of pigeonite, diopside, plagioclase, FeS, and metal. Small grains of FeS, metal, and clusters of olivine occur as inclusions in cumulus orthopyroxene. Overall characteristics are similar to those described in NWA 4215 [2], although **UAE 004** lacks compositional zoning in pyroxene and chromite. **NWA 2997** is similar to UAE 004 with the exception of having K-feldspar inclusions in chromite. We found that the vesicular **Dhofar 700** diogenite [2] also has chromite necklaces and a complicated thermal history that includes sector exsolution of clinopyroxene in orthopyroxene, partial resorption of primary, twinned orthopyroxene, and enclaves of polygonal recrystallized olivine (Figures 6, 7, 8, 9). The necklace mineral array in these specimens may have resulted from reaction between early-formed crystals and trapped intercumulus melt.

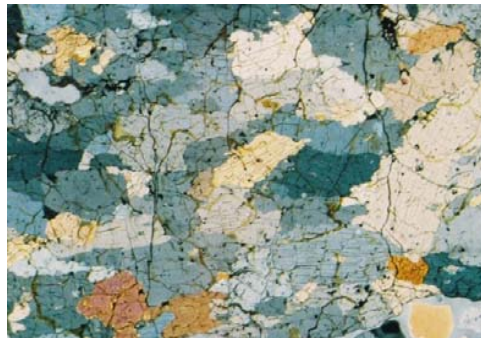


**Figure 4. UAE 004.** Linear orientation of orthopyroxene with irregular grain boundaries (lobate and sutured). Texture consistent with filter pressing compression and minor metamorphism. Base width = 14 mm; crossed polarizers.

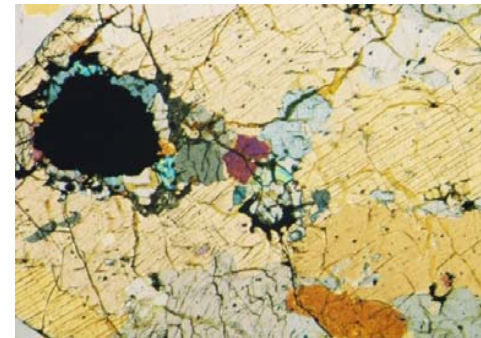


**Figure 5. UAE 004.** Precipitation or corona-like "necklace" around chromite. In addition, there are apparent relict islands of a primary orthopyroxene whose bulk was assimilated by a later generation of large orthopyroxene. Base width = 6 mm. Crossed polarizers.

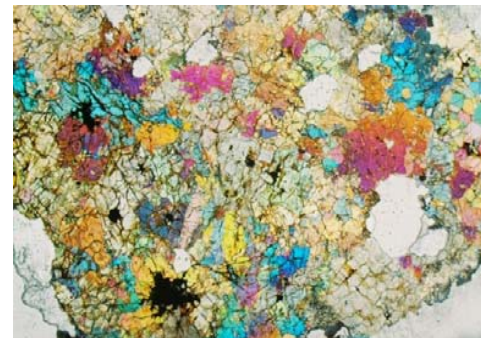


**Figure 6. Dhofar 700.** Large vesicles (up to 4 mm, blank areas), textural variations, and chromite with radiating offshoots (dark, lower left). Base width = 23 mm; partially crossed polarizers.

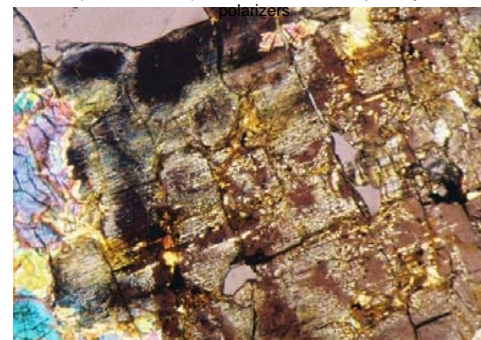


**Figure 7. Dhofar 700.** Crossed polarized light image of sector exsolution of clinopyroxene in orthopyroxene host. Base width = 6 mm.

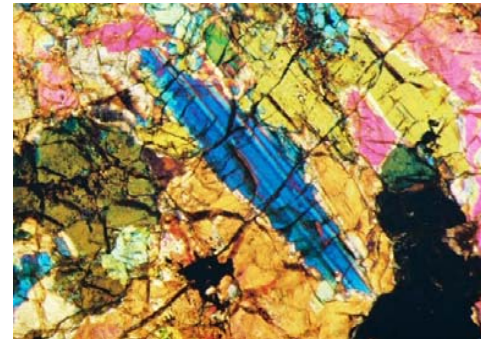


**Figure 8. Dhofar 700.** Partially resorbed, twinned orthopyroxene grain (blue) in a later generation orthopyroxene host. Base width = 4 mm; crossed polarizers.



**Figure 9. Dhofar 700.** Cluster of polygonal olivine (xenolith?) with partial poikilitic margin (right margin) of olivine chadacrysts and orthopyroxene host. Base width = 9 mm; crossed polarizers.

## Medium to coarse-grained (without corona-like "necklace" around chromites)

These specimens have simple mineralogy and contain > 95 vol % of orthopyroxene with sparsely distributed large subhedral chromite and traces of FeS and metal, e. g., **NWA 4654** (Figure 10). They are probably the unbrecciated equivalents to the "classic" diogenites mentioned above.

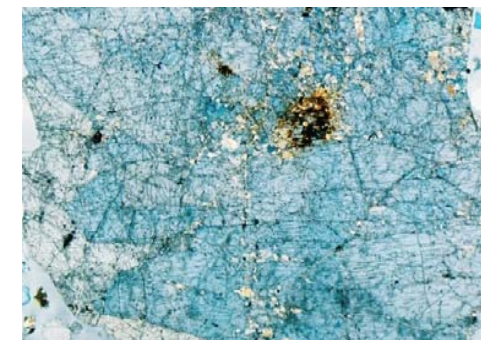


**Figure 10. NWA 4283.** Portion of a large, partially crushed, single orthopyroxene grain. Dark patch is oxide staining; smaller dark grains are chromite. Base width = 7 mm; partially cross-polarized light.

## Conclusions

From our preliminary observations, we conclude that crystallization of the various diogenite orthopyroxenites resulted from a range of differentiation mechanisms that include fractional crystallization (evidenced in most diogenites), replenishment (resorption textures, e. g., NWA 2039 and Dhofar 700), magmatic mixing and/or assimilation (xenolithic clusters in Dho 700), and possibly filter pressing (e. g., UAE 004 and NWA 2997). In time, it may turn out that the geological processes that acted on 4Vesta, aside from impact effects, are more complicated and advanced than we ever imagined. It will be most interesting to learn how the lithologies on 4Vesta identified by the DAWN mission compare not only with diogenites and olivine diogenites, but also with other meteorites including eucrites and mesosiderites, which share some mineralogical and isotopic characteristics with the specimens described here.

## References

- [1] Bunch T. E. et al. 2006 *MAPS*. [2] Barrat, J.-A. et al. 2006 *Met. Bull.* **90** [3] Mittlefehldt D. 1998 *Met. Bull.* **80 & 81**.